Antimicrobial resistance level and conjugation permissiveness shape plasmid distribution in clinical enterobacteria

Aida Alonso-del Valle[#,1,*], Laura Toribio-Celestino[#,1], Anna Quirant[2], Carles Tardio Pi[3,4], Javier DelaFuente[1], Rafael Canton[5,6], Eduardo Rocha[7], Carles Ubeda[2,8], Rafael Peña-Miller[3], Alvaro San Millan[1,8,*].

Affiliations

1. Centro Nacional de Biotecnología (CNB), CSIC. Madrid, Spain.

2. Fundación para el Fomento de la Investigación Sanitaria y Biomédica de la Comunitat Valenciana - FISABIO, Valencia, Spain.

3. Centro de Ciencias Genómicas, Universidad Nacional Autónoma de México, Cuernavaca, Mexico.

4. Instituto de Investigaciones en Matemáticas Aplicadas y en Sistemas, Unidad Académica Yucatán, Universidad Nacional Autónoma de México, Yucatán, México.

5. Servicio de Microbiología. Hospital Universitario Ramón y Cajal-IRYCIS. Madrid, Spain.

6. Centro de Investigación Biológica en Red de Enfermedades Infecciosas (CIBERINFEC), Instituto de Salud Carlos III, Madrid, Spain.

7. Institut Pasteur, Université de Paris Cité, CNRS UMR3525, Microbial Evolutionary Genomics, Paris, France.

8. Centro de Investigación Biológica en Red de Epidemiología y Salud Pública (CIBERESP), Instituto de Salud Carlos III, Madrid, Spain.

# Contributed equally

* Correspondence and request for materials should be addressed to Aida Alonso-del Valle (aalonso@cnb.csic.es) & Alvaro San Millan (asanmillan@cnb.csic.es).

Abstract

Conjugative plasmids play a key role in the dissemination of antimicrobial resistance (AMR) genes across bacterial pathogens. AMR plasmids are widespread in clinical settings, but their distribution is not random, and certain associations between plasmids and bacterial clones are particularly successful. For example, the globally spread carbapenem resistance plasmid pOXA-48 can use a wide range of enterobacterial species as hosts, but it is usually associated with a small number of specific *Klebsiella pneumoniae* clones. These successful associations represent an important threat for hospitalized patients. However, knowledge remains limited about the factors determining AMR plasmid distribution in clinically relevant bacteria. Here, we combined *in vitro* and *in vivo* experimental approaches to analyze pOXA-48-associated AMR levels and conjugation dynamics in a collection of wild type enterobacterial strains isolated from hospitalized patients. Our results reveal significant variability in these traits across different bacterial hosts, with *Klebsiella* spp. strains showing higher pOXA-48-mediated AMR and conjugation frequencies than *Escherichia coli* strains. Using experimentally determined parameters, we developed a simple mathematical model to interrogate the contribution of AMR levels and conjugation permissiveness to plasmid distribution in bacterial communities. The simulations revealed that a small subset of clones, combining high AMR levels and conjugation permissiveness, play a critical role in stabilizing the plasmid in different polyclonal microbial communities. These results help to explain the preferential association of plasmid pOXA-48 with *K. pneumoniae* clones in clinical settings. More generally, our study reveals that species- and strain-specific variability in plasmid-associated phenotypes shape AMR evolution in clinically relevant bacterial communities.

Significance statement

Conjugative plasmids disseminate AMR genes across bacterial pathogens. Understanding the rules governing plasmid dynamics in bacterial communities is therefore crucial to controlling the global AMR crisis. In this study, we analyzed the dynamics of an AMR plasmid of great clinical relevance, pOXA-48, in a collection of wild type bacteria recovered from hospitalized patients. We reported a high degree of variability in two key plasmid-associated phenotypes, AMR level and conjugation ability, across the collection of clinical bacteria. Using simulations based on the experimental results, we studied how successful associations between AMR plasmids and clinical

strains can arise in bacterial communities. Our results revealed that accounting for variability in plasmid-associated phenotypes help to understand the evolution of AMR in clinical settings.

Introduction

Plasmids shape bacterial ecology and evolution by spreading accessory genes across populations. Plasmids can disseminate both vertically and horizontally. Vertical transmission is coupled to the division of the bacterial host, whereas horizontal transmission is mediated mainly by conjugation (the direct cell-to-cell transfer of plasmids through a bridge-like connection) (1). Vertical plasmid transmission is favored in the presence of environmental stresses that select for plasmid-encoded genes, but in the absence of plasmid-specific selection, vertical transmission is usually hindered by the fitness costs that plasmids produce in their bacterial hosts (2, 3). Therefore, plasmids' interests can align or conflict with those of their bacterial hosts depending on the environmental conditions, leading to complex eco-evolutionary dynamics (4-6). Horizontal plasmid transmission can in principle make up for a deficit in vertical transmission, although conjugation rates vary considerably depending on the plasmid type (7, 8). The fate of plasmids in bacterial populations is thus determined by the interplay between horizontal and vertical transmission dynamics (and their evolution) (9-12). Multiple theoretical and experimental studies have investigated plasmid dynamics in clonal bacterial populations (examples can be found in 7, 8, 13-17). Other studies have analyzed the variability of plasmid-associated phenotypes across the diversity of wild type bacteria that plasmids encounter in natural communities (18-25). However, information remains very limited about how this variability may affect plasmid distribution in complex microbiota.

A dramatic example of the ability of plasmids to fuel bacterial evolution is the central role they play in the spread of antimicrobial resistance (AMR) in clinical pathogens, which is one of the most urgent public health threats facing humanity (26, 27). One particularly concerning group of drug resistant pathogens is carbapenemase-producing enterobacteria (order *Enterobacterales*), which appear on the WHO "priority pathogens" list (28, 29). Carbapenemases are β-lactamase enzymes able to degrade carbapenem antibiotics and are mainly acquired through conjugative plasmids (26). pOXA-48-like plasmids (from here on pOXA-48) constitute one of the most clinically important groups of carbapenemase-producing plasmids (30). pOXA-48 is a broad-host-

range conjugative plasmid from the plasmid taxonomic unit L/M (31) that encodes the OXA-48 carbapenemase and is disseminated across enterobacteria worldwide (30). Crucially, like most AMR plasmids, pOXA-48 is not randomly distributed across bacterial hosts. Although pOXA-48 has a broad potential host range, it is strongly associated with *Klebsiella pneumoniae* and is especially prevalent in high-risk clones of specific sequence-types (ST), such as ST11, ST307 or ST101 (32, 33). In a previous study, we proposed that this bias in host distribution could be explained in part by pOXA-48-associated fitness costs in the absence of antibiotics (34). We analyzed the distribution of pOXA-48 fitness effects across a collection of *Escherichia coli* and *Klebsiella* spp. clinical strains. Our results revealed that pOXA-48 produced a wide distribution of fitness effects across these hosts, but these effects could not explain overall plasmid distribution, especially at the species level (34).

In the present study, we investigate how other key plasmid-associated phenotypes determine pOXA-48 distribution across clinical enterobacteria. We determine pOXA-48-associated AMR level and conjugation permissiveness in a collection of multidrug resistant *E. coli* and *Klebsiella* spp. strains isolated from the gut microbiota of hospitalized patients. Through a combination of *in vitro* and *in vivo* experimental approaches, we demonstrate that (i) pOXA-48 confers a higher level of AMR in *Klebsiella* spp., and that (ii) *Klebsiella* spp. strains are, on average, more permissive than *E. coli* strains to pOXA-48 acquisition through conjugation. Finally, we integrate these new experimentally determined parameters with our previous fitness data in a simple population dynamics model. We use this model to interrogate the distribution of plasmid pOXA-48 in complex bacterial communities under different antibiotic concentrations.

Results

Experimental model system

In this study, we used a collection of multidrug-resistant clinical enterobacterial strains isolated from the gut microbiota of patients at a large hospital in Madrid, Spain (Ramon y Cajal University Hospital). We focused on the two most prevalent species associated with pOXA-48 in this hospital, *K. pneumoniae* and *E. coli* (32). Since *K. quasipneumoniae* and *K. variicola* (two species previously misidentified as *K. pneumoniae*) are also associated with pOXA-48 in the hospital (32),

118 we included strains from these species in the study. From now on we use *Klebsiella* spp. to refer
119 to the strains in our collection belonging to these three *Klebsiella* species.

120 To analyze pOXA-48 transmission dynamics it is necessary to work with pOXA-48-free strains,
121 which are able to receive the plasmid through conjugation. Therefore, we selected and sequenced
122 the genomes of 25 *Escherichia coli* and 25 *Klebsiella* spp. multidrug resistant strains that did not
123 carry this plasmid, and that were representative of the phylogenetic diversity of these species in
124 our hospital (Fig. S10 and Table S2, collection partially overlapping with the one in ref. (34), see
125 Methods). Although these strains were pOXA-48-naive, they were identified as ecologically
126 compatible with pOXA-48 because they were obtained from patients on hospital wards where
127 pOXA-48-carrying enterobacteria were commonly isolated during the same period (32, 34).

128 **AMR level conferred by pOXA-48 in wild type enterobacteria**

129 To characterize the fitness advantage associated with pOXA-48 in the presence of antibiotics, we
130 determined the impact of plasmid acquisition on the level of AMR. pOXA-48 was introduced by
131 conjugation into the pOXA-48-naive enterobacteria collection. Four *E. coli* strains and one *K.*
132 *pneumoniae* strain were unable to acquire the plasmid, and whole genome sequencing of the
133 remaining transconjugants revealed pOXA-48 mutations in six *E. coli* and six *Klebsiella* spp.
134 transconjugants. After excluding these strains, we used the remaining 15 *E. coli* and 18 *Klebsiella*
135 spp. isogenic strains pairs with or without pOXA-48 plasmid for this analysis (Fig. S10). For each
136 of the transconjugant (TC) and plasmid-free (PF) clones, we determined the minimal inhibitory
137 concentration (MIC) of 4 clinically important β-lactam antibiotics: amoxicillin in combination with
138 the β-lactamase inhibitor clavulanic acid (AMC) and the carbapenems ertapenem (ERT),
139 imipenem (IMP), and meropenem (MER) (Fig. 1A). Compared with *E. coli*, *Klebsiella* spp. strains
140 showed higher intrinsic resistance to all four antibiotics (Wilcoxon rank sum test: AMC, $W = 47.5$,
141 $P = 0.001$; ERT, $W = 14.5$, $P = 8.68 \times 10^{-6}$; IMP, $W = 15$, $P = 5.16 \times 10^{-6}$; MER, $W = 56$, $P = 0.002$),
142 as well as higher resistance level after plasmid acquisition (Wilcoxon rank sum test: AMC, $W =$
143 27, $P = 8.94 \times 10^{-5}$; ERT, $W = 82$, $P = 0.031$; IMP, $W = 29.5$, $P = 4.79 \times 10^{-5}$; MER, $W = 54$, $P =$
144 0.002).

145 The diverse genomic background and AMR gene content of the strains under study made it
146 difficult to elucidate a genetic origin for the higher AMR levels reached by pOXA-48-carrying

147 *Klebsiella* spp. (Fig. S11). However, a prominent influence on plasmid-mediated AMR level is
148 plasmid copy number (PCN). AMR level commonly escalates with PCN for AMR mechanisms
149 showing strong gene dosage effects, such as carbapenemases (35, 36). We used the genome
150 sequencing data to estimate pOXA-48 PCN in the strains under study (Fig. 1B). The results
151 showed that PCN was higher in *Klebsiella* spp. (mean = 2.21, SD = 1.53) than in *E. coli* strains
152 (mean = 1.41, SD = 0.55) (Wilcoxon rank-sum test, $W = 76$, $P = 0.03$). We then compared pOXA-
153 48 PCN and AMR levels for the antibiotic to which pOXA-48 confers the highest level of
154 resistance: AMC (average fold-change in MIC associated to pOXA-48 presence = 244.7, Fig.
155 S12). The final AMC resistance level correlated positively with PCN (Spearman's correlation: $R =$
156 0.5, $P = 0.003$; Fig. S13), supporting the idea that the higher PCN is at least partly responsible
157 for the elevated AMR level in *Klebsiella*. spp. Finally, to investigate if the differences in PCN were
158 also present in strains naturally carrying pOXA-48, we used the same genomic approach to
159 analyze PCN in a recently characterized large collection of 200 pOXA-48-carrying clinical isolates
160 from the same hospital. In line with the results from the transconjugant strains, PCN was higher
161 in *Klebsiella* spp. (mean = 2.35, SD = 0.88) than in *E. coli* (mean = 1.46, SD = 1.33) (Fig. 1C;
162 Wilcoxon rank-sum test, $W = 1271$, $P = 1.32 \times 10^{-14}$).

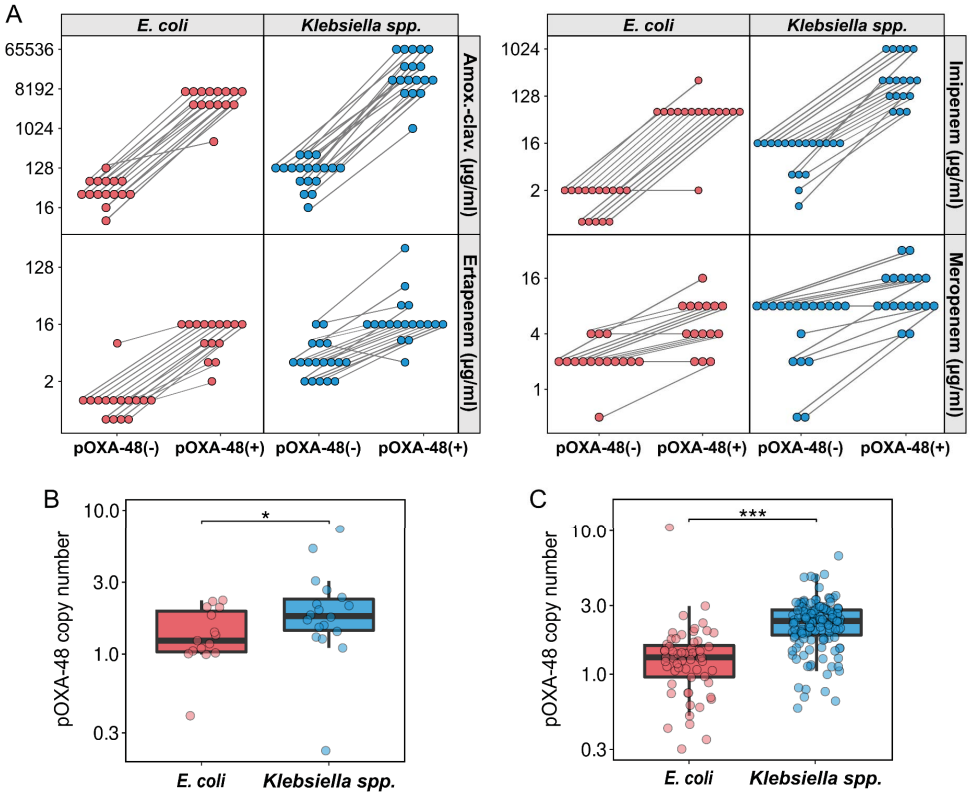

163

164 **Fig. 1. Resistance levels and copy number of pOXA-48 in wild type enterobacteria.** pOXA-
165 48 confers higher resistance levels and has a higher PCN in *Klebsiella* spp. than in *E. coli.* (A)
166 MIC (mg/L) of amoxicillin/clavulanic acid, ertapenem, imipenem and meropenem for the plasmid-
167 free/plasmid-carrying strain pairs (median of three biological replicates). (B) pOXA-48 plasmid
168 copy number (PCN) of the *E. coli* (n = 15) and *Klebsiella* spp. (n = 18) transconjugant strains.
169 PCN was estimated from sequencing data as the ratio of plasmid/chromosome median coverage
170 (see Methods). Horizontal lines inside boxes mark median values, the upper and lower hinges
171 correspond to the 25th and 75th percentiles, and whiskers extend to 1.5 times the interquartile
172 range. Dots indicate individual PCN values. To aid visualization, the y axis is represented in $\log_{10}$
173 scale with no value transformation. (C) pOXA-48 PCN in *E. coli* (n = 59) and *Klebsiella* spp. (n =
174 140) pOXA-48-carrying wild-type clinical strains. Boxplots are structured as in B. $^{*}P < 0.05$, $^{**}P$
175 < 0.01, $^{***}P < 0.001$.

176 **Conjugation frequency varies across clinical strains**

177 To analyze pOXA-48 horizontal transmission dynamics, we determined the ability of clinical
178 strains to acquire the plasmid by conjugation ("conjugation permissiveness"). For recipients, we
179 used a subset of 10 *Klebsiella spp.* and 10 *E. coli* strains representative of the genetic diversity
180 of the collection (Fig. S10). For donors, we used three pOXA-48-carrying strains. These were a
181 laboratory-adapted *E. coli* strain [β3914, a diaminopimelic acid (DAP) auxotrophic laboratory
182 mutant of *E. coli* K-12], and two wild-type pOXA-48-carrying clinical strains recovered from
183 hospitalized patients and belonging to STs responsible for between-patient plasmid dissemination
184 in the same hospital (32): *K. pneumoniae* ST11, and *E. coli* ST10 (strains K93 and C165
185 described in references 32 and 36).

186 We first performed classical conjugation assays (one donor and one recipient strain in equal
187 proportions) for all donor–recipient combinations, and measured conjugation frequencies as the
188 ratio between transconjugants (TC) and total recipient cells (see Methods for details). Note that
189 the donor *K. pneumoniae* ST11 could not be distinguished from three recipients of the same
190 species, either by the phenotype in the differential medium or by antibiotic selection, and therefore
191 conjugations could not be performed for these donor–recipient pairings. This analysis revealed a
192 wide diversity of conjugation frequencies across recipient strains. Overall, *Klebsiella spp.* strains
193 showed a significantly higher conjugation permissiveness than *E. coli* for all three donors (Fig.

194 2A, Kruskal-Wallis rank sum test: *E. coli* β3914, $X^2 = 45.8$, $P = 1.9 \times 10^{-11}$; *E. coli* ST10, $X^2 = 23.8$,
195 $P = 1.07 \times 10^{-6}$; *K. pneumoniae* ST11, $X^2 = 6.98$, $P = 8.24 \times 10^{-3}$). Moreover, two *E. coli* strains
196 produced no TCs with any of the donors, whereas all *Klebsiella spp.* strains produced TCs in at
197 least one of the conditions and were also the recipients with highest conjugation permissiveness
198 for every donor. Finally, we also calculated the conjugation rates from the mating assays with *E.*
199 *coli* ST10 as donor and the 20 recipient strains, using the end-point method (37) (Fig. S14).
200 Results ruled out the possibility that differences in growth dynamics of donors, recipients and TCs
201 could produce biases in the conjugation frequency results (37,38).

202 The gut microbiota is a dense bacterial community that engages in complex ecological
203 interactions. To analyze if community complexity could affect conjugation permissiveness in our
204 clinical strains, we repeated the conjugation assays, but this time instead of using a single clone
205 as the receptor, we used ten pairs of *E. coli*/*Klebsiella* spp. strains (Fig. 2B and Table S2). This
206 analysis once again revealed great variability in reception frequencies and a higher overall
207 conjugation permissiveness in *Klebsiella* spp. strains (Fig. 2B, paired Wilcoxon signed-rank exact
208 test: *E. coli* β3914, $V = 235$, $P = 0.017$; *E. coli* ST10, $V = 205$, $P = 0.01$; *K. pneumoniae* ST11, V
209 $= 45$, $P = 1.2 \times 10^{-4}$). In general, the conjugation frequencies observed agreed with those from
210 the single conjugation assays, suggesting that ecological interactions did not markedly affect
211 conjugation dynamics. However, one of the *E. coli* strains that produced no TCs as single receptor
212 was able to acquire the plasmid (PF_EC07), which could be due to secondary conjugations from
213 the *Klebsiella* spp. TC (39). Finally, to increase the complexity of the recipient community even
214 further, we performed conjugation assays using a pool of all 20 strains as recipients (Fig. 2C). In
215 this case, we could only distinguish between TCs at the species level in the differential medium.
216 Once again, the results revealed *Klebsiella spp.* to be more conjugation-permissive than *E. coli*,
217 regardless of the donor (Fig. 2C, Kruskal-Wallis rank sum test: *E. coli* β3914, $X^2 = 9.28$, $P = 2.32$
218 $\times 10^{-3}$; *E. coli* ST10, $X^2 = 9.31$, $P = 2.35 \times 10^{-3}$; *K. pneumoniae* ST11, $X^2 = 12.8$, $P = 3.49 \times 10^{-4}$).

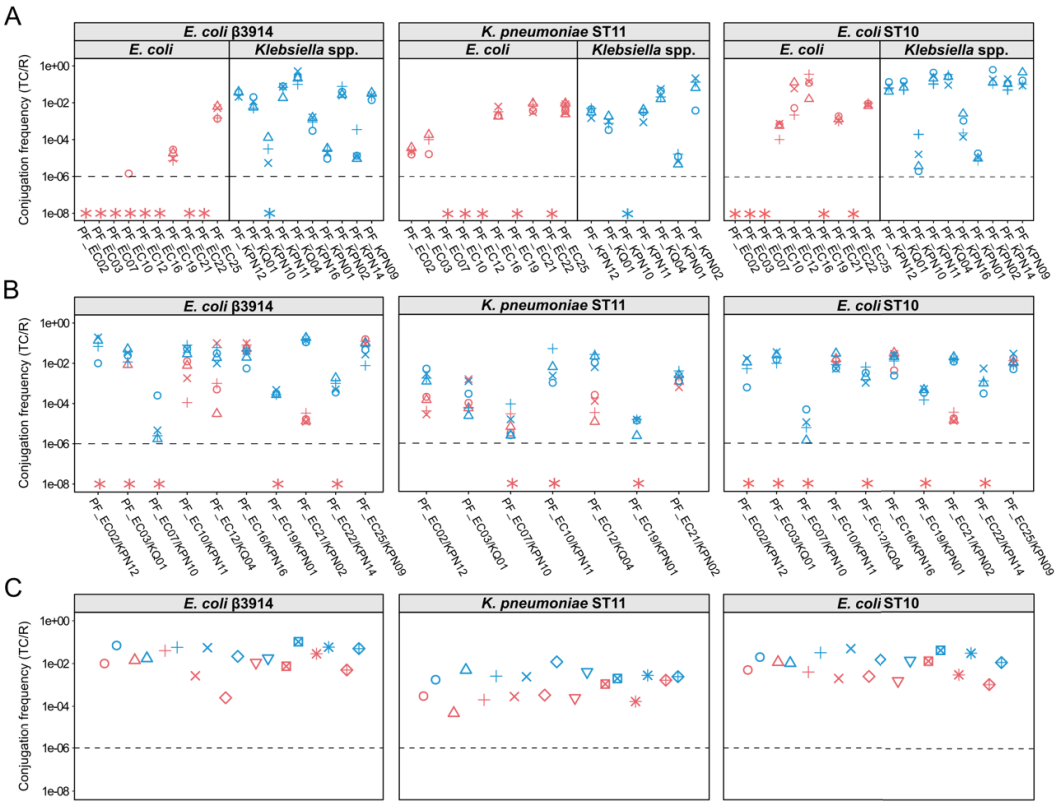

Fig. 2. *In vitro* pOXA-48 conjugation dynamics in wild type enterobacteria. Conjugation frequencies (transconjugants/recipient) of a subset of 20 isolates from our clinical enterobacteria collection (10 *E. coli* and 10 *Klebsiella* spp., x-axis), obtained from three pOXA-48 donors (*E. coli* β3914, left; *K. pneumoniae* ST11, center; and *E. coli* ST10, right). (A) Conjugation frequencies obtained in conjugation assays with one donor and one recipient in equal proportions. Color represents the recipient species (red, *E. coli*; blue, *Klebsiella* spp.), symbols represent biological replicates (n = 4), and asterisks symbolize conjugation frequencies below the detection limit (dotted line). *Klebsiella spp.* exhibits higher conjugation frequencies than *E. coli* for the three donors. (Kruskal-Wallis rank sum test: $P < 0.01$). (B) Conjugation frequencies using one donor and pairs of *E. coli* and *Klebsiella* spp. as recipients. *Klebsiella spp.* is more conjugation-permissive than *E. coli*, regardless of the donor used (Wilcoxon signed-rank exact test: $P < 0.01$). (C) Conjugation frequencies obtained with a pool of recipients (one donor, 20 recipients). The results give a conjugation frequency value per species, and symbols represent biological replicates (n=9) whose values would correspond to the most successful strains of each species in plasmid uptake. *Klebsiella spp.* has higher conjugation frequencies than *E. coli*, regardless of the donor (Kruskal-Wallis rank sum test: $P < 0.01$).

236 **Conjugation dynamics in a mouse model of gut colonization**

237 To contrast our *in vitro* results in a more biologically relevant environment, we studied pOXA-48
238 conjugation dynamics in a mouse model of gut colonization (C57BL/6J). As donor, we used *K.*
239 *pneumoniae* ST11 strain K93, since this clonal group is frequently responsible for gut microbiota
240 colonization of patients in our hospital (32). As recipients, we used 6 strains representative of the
241 variability in conjugation frequency observed *in vitro* (*E. coli* PF_EC10, PF_EC12, and PF_EC21;
242 and *Klebsiella spp*. FP_KQ01, PF_KPN11, and PF_KPN12). Mice (n = 21) were treated orally
243 with ampicillin (0.5 g/L), vancomycin (0.5 g/L), and neomycin (1 g/L) for one week to reduce
244 colonization resistance, as we previously described (40), and the antibiotic treatment was stopped
245 one day before inoculation. A total of 18 mice were inoculated orally with the donor and co-
246 inoculated 2 hours later with the recipients (3 mice per recipient), and 3 mice were not inoculated
247 with any bacteria, as controls. Fresh fecal samples were collected every 24 hours during 2 days.
248 At the end of the second day, mice were sacrificed, and cecum samples were collected. Samples
249 were processed and plated with antibiotic selection to determine colonization levels and the
250 frequency of transconjugants, as described in Methods. Two independent assays were
251 performed, two months apart, and the results of both assays are compiled below (Fig. 3 and
252 source data).

253 Colonization levels were high in all inoculated mice at both 24 and 48 hours for donor and recipient
254 strains (Fig. 3A), while no colonization was observed in the control mice. At 24 hours post-
255 inoculation, the numbers of transconjugants were generally low, and no differences in
256 transconjugant frequencies were detected between *E. coli* and *Klebsiella* spp. (Fig. 3B Kruskal-
257 Wallis rank sum test H = 1.4, P = 0.265). At 48 hours post-inoculation, the levels of donors were
258 similar in mice co-inoculated with *E. coli* or *Klebsiella* spp. recipient strains (Wilcoxon rank sum
259 test: in feces, W = 2.71, P = 0.1; in cecum, W = 0.1, P = 0.752). However, despite the fact that
260 the levels of *Klebsiella spp.* recipients were slightly lower than those of *E. coli* recipients (Wilcoxon
261 rank sum test: in feces, W = 245, P = 0.008; in cecum, W = 4.9, P = 0.026), *Klebsiella spp.* showed
262 significantly higher frequencies of transconjugants (Fig. 3B, Kruskal-Wallis rank sum test: in feces,
263 H = 24.6, P = 6.89 x 10^{-7}; in cecum, H = 10.2, P = 1.4 x 10^{-3}). In summary, the *in vivo* results
264 correlated qualitatively with those from the *in vitro* conjugation assays (Fig. 2A and 3B), and
265 *Klebsiella spp.* strains showed higher levels of transconjugants than *E. coli* strains on average.

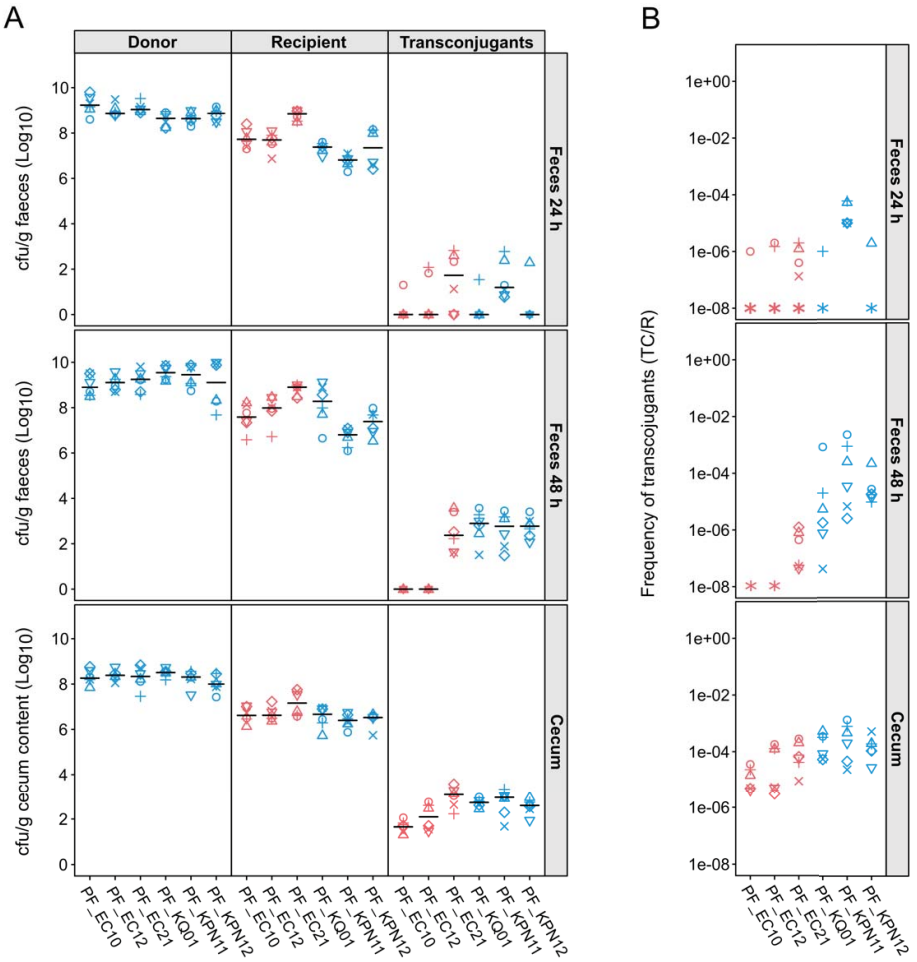

Fig. 3. pOXA-48 conjugation dynamics in a mouse model of gut colonization. pOXA-48 transconjugant frequencies in mouse feces and cecum at 24 and 48 hours post colonization. (A) Colonization levels of the donor (*K. pneumoniae* ST11), recipients (3 *E. coli* and 3 *Klebsiella spp.* strains), and transconjugants, in feces at 24 and 48 hours post-inoculation (top and center) and in cecum content at 48 h (bottom). Species are indicated by colors (red, *E. coli*; blue, *Klebsiella spp.*) and biological replicates (n=6) by symbols. Black lines indicate the median values for the biological replicates. Donor and recipient colonization levels were high in both feces and cecum. (B) Transconjugant frequencies (transconjugants/recipients) in feces at 24 and 48 hours (top and center) and in cecum (bottom). Transconjugant frequencies were significantly higher in *Klebsiella* spp. than in *E. coli* in both feces and cecum at 48 hours (Kruskal-Wallis rank sum test in feces H = 24.6, $P = 6.89 \times 10^{-7}$; in cecum H = 10.2, $P = 1.4 \times 10^{-3}$).

279 **Simulating plasmid-host associations in complex populations**

280 We previously developed a mathematical model to study how pOXA-48 fitness effects impact
281 plasmid maintenance in complex bacterial communities (34). That model allowed us to predict
282 the competitive fitness of each strain, with and without pOXA-48, based on growth-kinetic
283 parameters that were calibrated from experimental growth curves obtained from single clones. In
284 the present study, we extended this model to include the new variables informed by the
285 experimental results: conjugation permissiveness and resistance levels (Fig. 4A,B). Specifically,
286 we used the conjugation rates values obtained using *E. coli* ST10 as donor, and resistance levels
287 to AMC (see Supporting Information for a complete description of the model and its
288 parametrization). This computational model allowed us to track the distribution of plasmids in
289 response to selection at species and strain resolution.

290 We first simulated simple pairwise competition experiments between the 10 *Klebsiella* spp. and
291 10 *E. coli* strains in our collection with experimentally determined conjugation rates and AMR
292 levels (Table S1). Each competition experiment started with a 1:1 ratio, and a 50% plasmid
293 frequency in each strain (see Supporting Information). To assess the role of antibiotics in the
294 distribution of plasmids in the population, we performed all pairwise competition experiments for
295 a range of selective pressures (Fig. S5-S7). At low and intermediate antibiotic concentrations, the
296 plasmid was preferentially associated with *E. coli*. In contrast, as the selective pressure increased,
297 the proportion of plasmid-carrying *Klebsiella* spp. strains within the pairs correspondingly
298 increased, reflecting the relatively lower resistance levels exhibited by *E. coli* strains (Fig. S5-S7).

299 We next used the model to analyze the impact of AMR levels and conjugation permissiveness in
300 pOXA-48 distribution in complex communities, such as those in the gut microbiota of hospitalized
301 patients (Fig. 4 and S8). Our previous epidemiological studies revealed that patients are
302 commonly colonized by pOXA-48-carrying nosocomial enterobacterial clones (32). During
303 colonization, the plasmid spreads horizontally to resident enterobacteria in the gut, and different
304 clones can subsequently maintain the plasmid in the community, producing long term pOXA-48
305 gut carriage (32). To simulate the invasion and dissemination within the gut microbiota
306 community, we used our mathematical model to initialize multistrain simulations with only one
307 member of the community carrying pOXA-48 (starting at a frequency of 0.01% of the total density,

308 Fig. 4A,B). We conducted 10-day simulated serial dilution experiments with a starting community
309 including the 20 strains (the 10 *E. coli* and 10 *Klebsiella spp.*). We then explored the effects of
310 various antibiotic concentrations on community compositions (Fig S8), aiming to evaluate the
311 plasmid dynamics and to identify the successful associations between plasmid and hosts. At low
312 drug concentrations, we found that, as the selective pressure increases, the population shifts from
313 being dominated by plasmid-free *E. coli* to contain mostly plasmid-free *Klebsiella* spp. (Fig. 4C).
314 At intermediate and high drug concentrations, plasmid-carrying strains dominate, with only
315 *Klebsiella* spp. strains being able to persist at very high concentrations. At the strain-level, the
316 simulations revealed that the species-level dynamics were driven by a small subset of successful
317 strains, which played a key role in stabilizing the plasmid in the communities (Figs 4D). At
318 intermediate and high drug concentrations, plasmid-carrying PF_KPN12 (ST307), PF_EC02
319 (ST453), and PF_KPN11 (ST307) were the most prevalent strains. At very high antibiotic
320 concentrations pOXA-48-carrying PF_KPN11 (ST307) clearly dominated the population.

321 Finally, we followed a different approach to further evaluate if specific bacterial strains played an
322 important role in maintaining plasmid stability within the community. We used an iterative knock-
323 out simulation approach where strains were sequentially and randomly removed from the 20-
324 strain community, with an evaluation of plasmid stability after each removal. This approach
325 revealed the important role of strains PF_EC03 (ST131), PF_EC16 (ST38), PF_KPN11 (ST307)
326 in antibiotic-free environments (Fig. S9). In high-antibiotic-concentration environments,
327 PF_KPN02 (ST485), PF_KQ01, and again, PF_KPN11 (ST307) played key roles in maintaining
328 plasmid stability (Fig S9).

329 Taken together, our results underscore the critical role of successful plasmid-host associations in
330 securing plasmid stability in mixed microbial populations. Specifically, we observed that certain
331 strains in our pool, such as PF_KPN11 (ST307), are crucial for the dissemination and
332 maintenance of plasmid pOXA-48 in the communities.

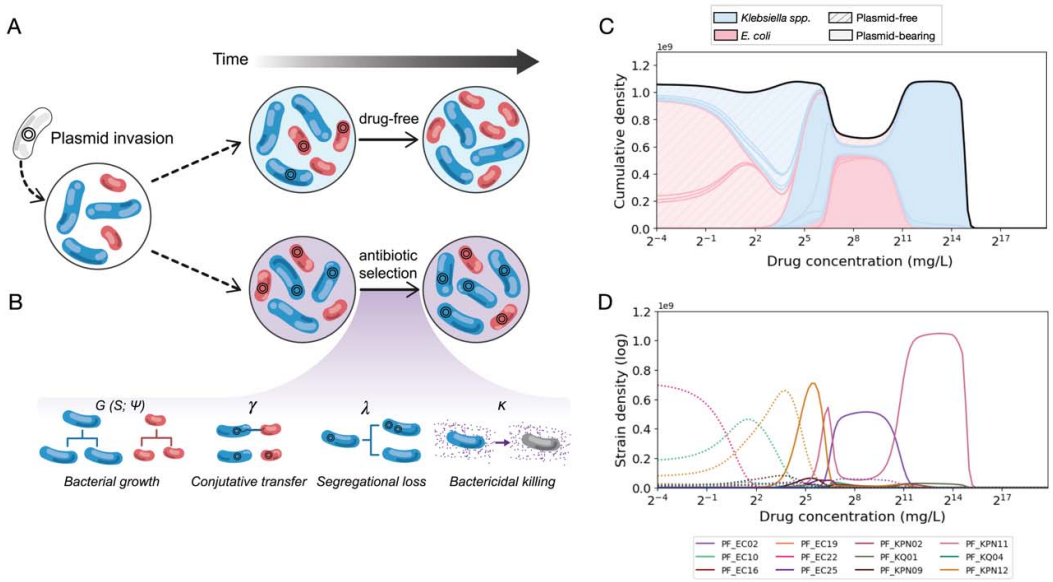

Fig. 4. Computational model of plasmid population dynamics. (A) Diagram illustrating the computational approach employed to assess the distribution of plasmids within mixed bacterial populations under a range of selective pressures (see Supporting Information). (B) The model simulates various ecological processes that influence plasmid dynamics, enabling the exploration of their behavior under different conditions, including bacterial growth, modeled as a Monod term G (S; ψ), conjugative transfer occurring at a rate γ, segregational loss occurring at a rate λ, and antibiotic bactericidal killing κ (Table S1). (C) Population dynamics simulated across a range of drug concentrations, starting with an initial population of 10 *E. coli* and 10 *Klebsiella* spp. strains. Predominantly, plasmid-free bacteria emerge at low drug levels, while plasmid-bearing *Klebsiella* spp. prevail under high drug concentrations. (D) Strain-level resolution in the simulations of the multistrain dose-response. In conditions of low drug concentrations, the plasmid-free strains PF_EC22 (ST131) and PF_KPN12 (ST307) are predominant. In high drug concentration environments, the strain PF_KPN11 (ST307) appears to contribute to the preservation of plasmid stability in these communities.

Klebsiella*-derived capsules are associated with plasmid carriage in *E. coli

The conjugation experiments showed a higher permissiveness for pOXA-48 acquisition in *Klebsiella* spp. than in *E. coli*, as well as high variability between strains of the same species. We sought to investigate the genetic traits that could explain these differences. We analyzed the

352 genomes of the 20 recipient strains for an array of traits known to affect conjugation efficiency:
353 CRISPR arrays, restriction-modification (RM) systems and other phage defense systems that
354 could target pOXA-48, plasmid incompatibilities, and type VI secretion systems (T6SS, known to
355 mediate bacterial competition, which may affect conjugation frequencies). However, none of
356 these traits accounted for the observed differences in pOXA-48 acquisition (Fig. S15, Table S3).

357 Capsules have been reported to hinder DNA transfer and possibly constitute a barrier to plasmid
358 acquisition (41, 42). We used two software tools to search for capsular systems: Kaptive, to detect
359 and type *Klebsiella* capsular loci, and CapsuleFinder, to identify other capsular systems. With the
360 single exception of the non-capsulated PF_KPN14 strain, each recipient strain encoded a specific
361 set or type of complete capsular loci (Table S3). To assess whether similar sets of capsular loci
362 were associated with higher or lower conjugation permissiveness, we calculated a weighted gene
363 repertoire relatedness (wGRR) score. Although we found no clear pattern for the *Klebsiella* spp.
364 recipients, the *E. coli* strain with the highest overall pOXA-48 reception permissiveness across
365 the three different donors, PF_EC25, encoded a *Klebsiella* capsular locus (KL35, Fig. 5A, Table
366 S3).

367 To determine if *Klebsiella*-derived capsules better facilitate pOXA-48 acquisition than other
368 capsular systems, we analyzed their association in the complete genomes of 1,585 *E. coli* and
369 715 *K. pneumoniae* strains (RefSeq), of which 6 *E. coli* strains and 46 *K. pneumoniae* strains
370 carry pOXA-48 (Fig. 5B, Table S4). We used phylogenetic logistic regression (*phyloglm*) to
371 account for phylogenetic dependency of the significant associations ($P < 0.05$, Fisher's exact test;
372 Table S6). The presence of *Klebsiella*-derived capsules was associated with pOXA-48 carriage
373 only when *E. coli* and *K. pneumoniae* were analyzed together (Table S6, *phyloglm* $P = 0.0016$).
374 We next investigated the relationship between the presence of *Klebsiella*-derived capsules and
375 plasmid carriage more generally, finding significant associations when analyzing *E. coli* and *K.*
376 *pneumoniae* together (Table S6, *phyloglm* $P < 2 \times 10^{-16}$) and when analyzing *E. coli* separately
377 (Table S6, *phyloglm* $P = 2.2 \times 10^{-5}$). Moreover, *E. coli* strains encoding other capsular systems
378 (not derived from *Klebsiella*) were more likely to be plasmid-free or to carry only one plasmid,
379 whereas *E. coli* encoding *Klebsiella*-derived capsules had an increased likelihood of carrying
380 multiple plasmids (Fig. 5C). These results suggest that although capsules generally obstruct

conjugation (41, 42), certain types of *Klebsiella*-derived capsules could be more permissive than other capsule types to plasmid acquisition by *E. coli*.

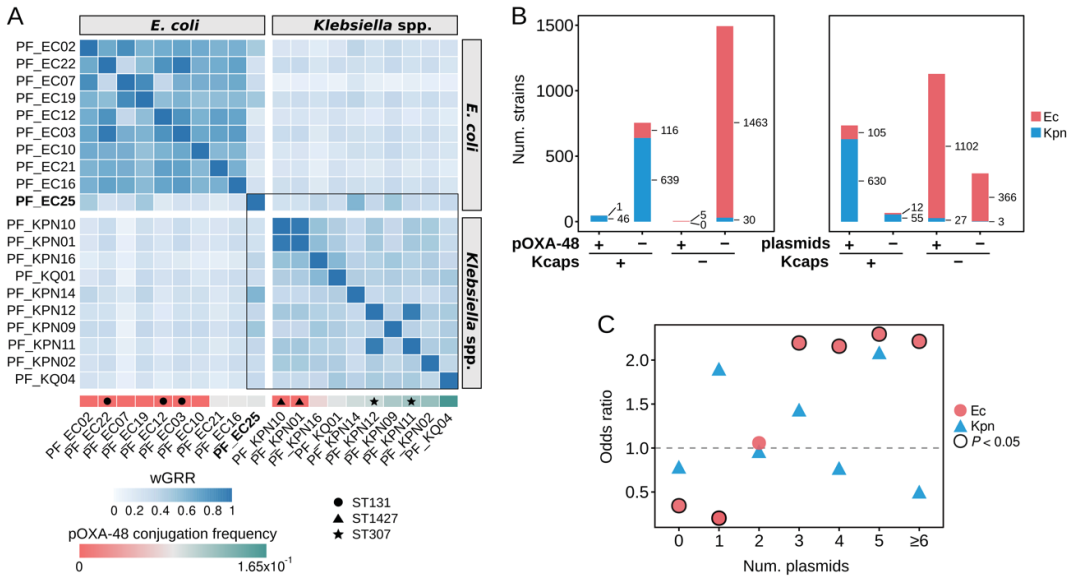

Fig. 5. Associations between capsular systems and plasmid carriage. Analysis of capsular systems and plasmid prevalence in our recipient strains and in *E. coli* and *K. pneumoniae* genomes obtained from RefSeq. (A) Heatmap of weighted gene repertoire relatedness (wGRR) scores between capsular sets (*Klebsiella*-derived capsules and/or other capsular systems) encoded by the recipient strains used in conjugation experiments. A wGRR score of 1 means that all proteins from the capsular set encoding the fewest number of proteins have a homolog in the capsular set it is compared with. A score of 0 indicates there are no homologs between the capsular sets of the two compared strains. Recipients are ordered by median pOXA-48 conjugation frequency across replicates and donors. The PF_EC25 strain, highlighted in bold, has the highest median conjugation frequency of any *E. coli* strain and is the only *E. coli* strain encoding a *Klebsiella*-derived capsule. Strains from the same sequence type (ST) are marked with a symbol. The black square indicates strains with a *Klebsiella*-derived capsule. (B) Number of *E. coli* (Ec) and *K. pneumoniae* (Kpn) strains from the RefSeq database analyzed for the association between the presence of *Klebsiella*-derived capsules (Kcaps) and carriage of pOXA-48 (left) or plasmids in general (including pOXA-48; right). In total, the RefSeq database includes 1,585 Ec and 715 Kpn strains. (C) Association between the presence of a genome-encoded *Klebsiella*-derived capsule and the number of plasmids carried in the *E. coli* (Ec) and *K. pneumoniae* (Kpn) RefSeq strains. The chart shows odds ratio (Fisher's exact test) of plasmid

402 carriage for strains encoding a *Klebsiella*-derived capsule *vs* strains encoding other capsular
403 systems (not from *Klebsiella*). Values above 1 (horizontal dashed line) indicate a positive
404 association, and values below 1 a negative association, between encoding *Klebsiella*-derived
405 capsules and carrying the indicated number of plasmids. In all cases, the number of strains
406 carrying each number of plasmids is >100. A significant Fisher's test ($P < 0.05$) is indicated by a
407 black outline.

408 **Discussion**

409 In this work, we performed a comprehensive analysis of pOXA-48 effects in clinical
410 enterobacteria. One of the main strengths of this study is the relevance of the experimental
411 system. We used an epidemic carbapenem resistance plasmid, pOXA-48, and a collection of
412 wild-type, multidrug resistant, enterobacterial isolates recovered from hospitalized patients. Using
413 this system, we analyzed pOXA-48-associated AMR levels and conjugation permissiveness both
414 *in vitro* and *in vivo* (Figs. 1-3). The key advantage of experimentally determining plasmid-
415 associated phenotypes in a collection of wild type clinical enterobacteria is that we can confidently
416 feed these variables into mathematical models. We developed a model including three key
417 variables informed by our experimental results: bacterial growth dynamics with and without pOXA-
418 48 (34), conjugation permissiveness (Fig. 2 and S14), and AMR levels (Fig. 1). We used this
419 model to investigate pOXA-48 dynamics in complex bacterial communities under different levels
420 of selection, aiming to simulate pOXA-48 invasion of a gut microbiota (Fig. 4).

421 The critical result of our study is that pOXA-48-associated phenotypes vary significantly across
422 different wild type bacterial hosts. We had previously shown that pOXA-48 produces variable
423 fitness effects in the absence of antibiotics (34, 43), and in this new study we reveal similar
424 variability in pOXA-48-associated AMR levels and conjugation permissiveness. This variability is
425 especially evident for horizontal transmission, with conjugation frequencies differing by orders of
426 magnitude across different recipients. Our simulations revealed that the variability of plasmid-
427 associated phenotypes dramatically impact plasmid distribution in polyclonal bacterial
428 communities. Specifically, a single successful pOXA-48-bacterium association is sufficient to
429 allow for plasmid invasion and stable maintenance in a complex population for a wide range of
430 antibiotic concentrations (Fig. S8). These jackpot associations, combining high growth rates, high
431 AMR levels, and high conjugation permissiveness, can act as pOXA-48 super-sinks in the gut

432 microbiota of patients, maintaining and further disseminating the plasmid. Interestingly, these
433 successful pOXA-48-carrying clones are likely to produce long-term colonization of the gut
434 microbiota of patients, as we have recently reported (32). Long-term colonization may in turn lead
435 to the dissemination of carbapenemases from clinical settings towards the community, which
436 represents a critical step in AMR epidemiology.

437 One of the main goals of this study was to understand the bias in pOXA-48 distribution across
438 enterobacteria. Despite having a broad host range and producing similar fitness effects in *E. coli*
439 and *Klebsiella* spp. (34, 43), pOXA-48 is usually associated with specific *K. pneumoniae* clones
440 in hospitals (32, 33). Our results help to explain this bias. We experimentally showed that,
441 compared with *E. coli*, *Klebsiella* spp. clones generally have a higher AMR level associated with
442 pOXA-48 carriage and a greater ability to take up pOXA-48 by conjugation. Crucially, our
443 simulations of both pairwise competitions and complex bacterial communities revealed that
444 pOXA-48 is mostly associated with *Klebsiella* spp. under high antibiotic pressure. Taken together,
445 these results help to explain why pOXA-48 is usually associated with *K. pneumoniae* in the gut
446 microbiota of hospitalized patients, which is a complex community frequently exposed to high
447 antibiotic pressure. At the strain level, our model also provides interesting information. The most
448 relevant result emerging from our simulations is that *K. pneumoniae* strains belonging to ST307
449 (PF_KPN12 and specially PF_KPN11) are responsible for pOXA-48 maintenance in the bacterial
450 communities. Importantly, ST307 is a clonal group that is emerging as major cause of nosocomial
451 outbreaks in many different regions around the world, and is usually associated with plasmid-
452 mediated extended-spectrum ß-lactamases (ESBLs) and carbapenemases (33, 44, 45). In Spain,
453 ST307 is actually becoming the most concerning pOXA-48-carrying clonal group in hospitals,
454 replacing other high-risk *K. pneumoniae* STs, such as ST11 (32, 46). Therefore, our simulations
455 based on data obtained from clinical strains which were originally pOXA-48-free were able to
456 mirror the real dynamics observed in our hospital. These results suggest that the experimentally
457 determined phenotypes: fitness with and without plasmid, AMR levels and conjugation
458 permissiveness, could help to predict the evolution of plasmid-mediated AMR in clinical settings.

459 Given the importance of the variability of plasmid-associated phenotypes in the evolution of
460 plasmid-mediated AMR, a critical research direction in the field will be to characterize the
461 molecular basis underlying these differences. In this study, we showed that the presence of

462 *Klebsiella*-derived capsules, compared to other capsular systems, is associated with a higher
463 plasmid frequency in an *E. coli* clone (Fig. 5). We also showed that pOXA-48 PCN is higher in
464 *Klebsiella* spp. than in *E. coli* clones, probably contributing to the higher AMR level observed in
465 pOXA-48-carrying *Klebsiella* spp. strains (Fig. 1). Further work will be needed to characterize the
466 molecular basis and significance of these and other specific interactions. Understanding the
467 plasmid and host factors that determine this variability will help us not only to predict, but also
468 hopefully to counteract successful associations between AMR plasmids and high-risk bacterial
469 clones.

470

471 **Methods**

472 **pOXA-48_K8 plasmid, strains, and growth conditions.** We used 50 wild type pOXA-48-free
473 enterobacterial strains recovered from the gut microbiota of hospitalized patients (Table S2,
474 partially overlapping the collection in (34)). These strains belonged to the R-GNOSIS collection,
475 which was constructed in our hospital during an active surveillance-screening programme for
476 ESBL/carbapenemase-producing enterobacteria (from March 4th, 2014 to March 31st, 2016, R-
477 GNOSIS-FP7-HEALTH-F3-2011-282512,
478 https://cordis.europa.eu/project/id/282512/reporting/es, approved by the Ramón y Cajal
479 University Hospital Ethics Committee, Reference 251/13). These strains are representative of *E.*
480 *coli* and *Klebsiella* spp. diversity in the R-GNOSIS collection, and we define them as ecologically
481 compatible with plasmid pOXA-48, because they were obtained from patients on hospital wards
482 where pOXA-48-carrying enterobacteria were commonly isolated during the same period. To
483 analyze the pOXA-48-associated AMR level, we selected 33 isogenic strains pairs (15 *E. coli* and
484 18 *Klebsiella* spp.) with (TC) or without pOXA-48 plasmid (PF) from the collection. Plasmid-
485 bearing strains carry the most common pOXA-48-like plasmid variant from our hospital, pOXA-
486 48_K8 (32). For the conjugation frequencies determination, we selected, as recipients, 10 *E. coli*
487 and 10 *Klebsiella spp.* pOXA-48-free isolates that cover the phylogenetic diversity of the collection
488 (Fig. S10) (32) and showed similar β-lactam resistance levels. As plasmid donors we selected
489 three pOXA-48_K8-carrying strains: *E. coli* β3914 (47), *K. pneumoniae* K93, and *E. coli* C165 (32,

490 36). Bacterial strains were cultured in LB at 37 °C with continuous shaking (250 r.p.m), and on LB
491 or HiCrome™ UTI (Himedia Laboratories, India) agar plates at 37 °C.

492 **Determination of minimum inhibitory concentration (MIC).** We determined the MIC of AMC
493 (Normon, Spain), ERT (Merck Sharp & Dohme B.V., Netherlands), IMP (Fresenius Kabi,
494 Germany) and MER (SunPharma, India) in all plasmid-carrying and plasmid-free clones selected
495 for this study following a modified version of the agar dilution protocol (48, 49). This method allows
496 us to test a large number of isolates simultaneously under identical conditions and to test a wide
497 range of AMC concentrations, since this β-lactam antibiotic degrades fast in liquid medium (50).
498 We prepared pre-cultures of plasmid-free and plasmid-carrying strains by inoculating single
499 independent colonies into LB broth in 96-well plates and overnight incubation at 37 ºC with
500 continuous shaking (250 r.p.m.). We spotted 10 µl of each overnight culture onto LB agar plates
501 with increasing concentrations of AMC (from 4 mg/L to 32,768 mg/L), ERT (from 0,25 mg/L to 512
502 mg/L), IMP (from 0.25 mg/L to 1,024 mg/L) or MER (from 0.25 mg/L to 32 mg/L), and incubated
503 them overnight at 37 ºC. We determined the MIC of each strain as the lower antimicrobial
504 concentration able to inhibit the growth of each strain. We performed three biological replicates
505 per MIC determination in three independent days, and we used the median value of the three
506 replicates as the MIC.

507 ***In vitro* determination of conjugation frequencies and rates.** To determine the *in vitro*
508 conjugation frequencies, we selected, as recipient strains, 10 *E. coli* and 10 *Klebsiella spp.* pOXA-
509 48-free isolates, from our collection of ecologically compatible enterobacterial isolates (Fig. S10).
510 As plasmid donors we used three pOXA-48_K8-carrying strains: *E. coli* β3914, a counter-
511 selectable diaminopimelic acid auxotrophic laboratory strain (47); *K. pneumoniae* K93, a pOXA-
512 48-carrying ST11 strain; and *E. coli* C165, a pOXA-48-carrying ST10 strain (32, 36). To counter-
513 select the two natural donors, we transformed the recipients with pBGC plasmid, a non-
514 mobilizable *gfp*-carrying small plasmid that encodes a chloramphenicol resistance gene (34). It
515 was not possible to introduce pBGC into three *Klebsiella spp.* isolates (PF_KPN09, PF_KPN14 y
516 PF_KPN16), due to their level of constitutive resistance to chloramphenicol. We streaked donor
517 and recipient strains from freezer stocks onto LB agar plates with or without ertapenem 0.5 mg/L
518 –and 0.3 mM DAP for *E. coli* β3914/pOXA-48_K8–, respectively, and incubated at 37 °C
519 overnight. We prepared pre-cultures of donors and recipients by inoculating single independent

520 colonies in 15-ml culture tubes containing 2 ml of LB broth and overnight incubation at 37 ºC with
521 continuous shaking (250 r.p.m.). To perform classic conjugation assays, we mixed one donor and
522 one recipient at equal proportions (each donor with each recipient, independently, with a total of
523 4 recipient biological replicates by donor), plated the mixture as a drop onto LB agar plates –
524 supplemented with DAP 0.3mM for *E. coli* β3914/pOXA-48_K8 donor– and incubated them at 37
525 ºC during only 4h. A short mating experiment (4 hours) reduces the chances of secondary
526 conjugation events from transconjugants to recipients, but we cannot rule out this possibility. Also,
527 4 hours mating reduces the impact of potential differences in donor, recipient, and transconjugant
528 growth rates on conjugation frequency determination. After incubation, we collected the biomass,
529 resuspended it in 1 ml of NaCl 0.9 % and performed 1/10 serial dilutions up to 10^{-6}. We estimated
530 the final densities of transconjugants and recipients by plating 10 µl of each dilution on HiCrome™
531 UTI agar plates (HIMEDIA laboratories, India) with or without AMC 256 mg/L, respectively, and
532 with chloramphenicol 50 mg/L. We plated the dilutions as drops, and each drop was subsequently
533 allowed to drain down the plate, this way we can separate the colonies so they are easily
534 distinguishable and quantifiable. We performed the donor counter-selection by the absence of
535 DAP in the medium for *E. coli* β3914/pOXA-48_K8, or by selection with chloramphenicol for
536 clinical *K. pneumoniae* ST11 and *E. coli* ST10. Finally, we calculated the conjugation frequencies
537 per recipient following the formula below:

538 $$Conjugation\ frequency_R = \frac{CFU_{transconjugants}}{CFU_{recipient}}$$

539 where $CFU_{transconjugants}$ are the transconjugant colony-forming units obtained from the number of
540 colonies in the plate (corrected by the dilution factor); and $CFU_{recipient}$ are the number of recipient
541 colony-forming units minus transconjugants. Note that in the cases where no TC colonies were
542 detected in the plate, we calculated a threshold conjugation frequency assuming the presence of
543 a single colony in the total cell suspension, thus establishing a detection limit of 10^{-6}. Conjugation
544 rates were calculated for the experiments performed using *E. coli* ST10 as a donor and the 20
545 recipient strains. For these mating experiments, the number of donors, recipients and
546 transconjugants were determined both before and after the mating assays as described above,
547 and the conjugation rates were determined using the end-point method for solid surfaces (37).

548 To perform conjugation assays with recipient pairs we randomly grouped the recipients in pairs
549 so that each pair comprised one *E. coli* and one *Klebsiella spp.* recipient. We used a modified
550 version of the above protocol, in which we mixed recipient pre-cultures of each pair at equal
551 proportions and we subsequently mixed these recipient mixtures with the pre-culture of the donor
552 at the same proportion, forming the final conjugation reaction (each recipient pair with one donor
553 per time, with 4 biological replicates of recipient pairs). We determined the recipients and
554 transconjugants densities by antibiotic selection with AMC 256 mg/L, (to select transconjugants
555 vs. recipients) and chloramphenicol 50 mg/L (to counter-select donors), and distinguished
556 between recipients using the differential chromogenic medium HiCrome™ UTI agar. We
557 calculated the conjugation frequency per each receptor using the formula above.

558 For conjugation assays with a pool of all the recipients, we mixed the same pre-culture volume of
559 all recipient strains with one donor per experiment, following the same protocol previously
560 described. Nine biological replicates were performed.

561 ***In vivo* conjugation.** For the determination of conjugation frequencies of clinical isolates *in vivo*,
562 we performed conjugation assays using a mouse model of gut colonization. We selected a subset
563 of 6 pBGC-carrying recipient strains from the *in vitro* conjugation assays: 3 *E. coli* (PF_EC10,
564 PF_EC12 and PF_EC21) and 3 *Klebsiella spp.* (PF_KQ01, PF_KPN11 and PF_KPN12) strains.
565 As plasmid donor we selected the natural pOXA-48_K8-carrying isolate, *K. pneumoniae* ST11,
566 K93 (32). We carried out the experiment described below twice, 2 months apart and under
567 identical conditions.

568 *Mouse model and housing conditions*. We used 6-week-old C57BL/6J female mice (n =
569 21) purchased from Charles River Laboratories and housed them with autoclave-sterilized food
570 (a 1:1 mixture of 2014S Teklad Global diet and 2019S Teklad Global Extrused 19% Protein
571 Rodent Diet from Envigo) and autoclave-sterilized water. Temperature was kept at 21 ± 2 °C and
572 humidity was maintained at 60–70%, in 12 h light/dark cycles. To allow intestinal colonization of
573 the donor and recipient strains, we disrupted the intestinal microbiota by administering ampicillin
574 (500 mg/L), vancomycin (500 mg/L) and neomycin (1 g/L) in the drinking water for one week, as
575 previously described (40). Water with antibiotics was changed every 3-4 days to avoid reduction
576 of antibiotic activity. During antibiotic treatment, mice were co-housed (3-6 mice per cage). After

577 1 week of treatment, antibiotics were removed from the drinking water and mice were individually
578 housed to avoid bacterial transfer between mice due to coprophagia during the experiment.

579 *Mice inoculation with donor and recipient strains.* 1 day after antibiotic treatment removal,
580 18 out of 21 mice were inoculated by oral gavage with 10^7 CFU of the donor strain, *K. pneumoniae*
581 ST11. Two hours later, each donor-inoculated mouse was co-inoculated by oral gavage with 10^7
582 CFU of a recipient strain (3 mice per recipient). This way, from the initial 21 mice, 18 of them were
583 inoculated with donor and recipient bacteria (6 different recipients, 3 mice per recipient) and 3
584 mice remained uninoculated as control.

585 *Sample collection and bacterial levels determination.* After antibiotic treatment and prior
586 to inoculation, we collected fresh fecal samples from each mouse as to control for the absence of
587 bacteria able to grow on the selective medium used for our bacteria of interest. We weighted the
588 feces and resuspended them in 1 ml PBS until a homogeneous mixture was obtained. Then, we
589 diluted mixtures 1:100,000 and plated 100 µl on HiCrome$_{TM}$ UTI agar plates with ampicillin (400
590 mg/L) and vancomycin (1 mg/L). We incubated the plates overnight at 37 ºC. After incubation,
591 bacterial growth was found to be absent. During the assay, we collected fresh fecal samples from
592 each mouse 24 and 48 h post inoculation and processed samples as described before. To
593 determine the donor, recipients and transconjugants densities, we plated 100 µl of different
594 dilutions onto HiCrome$_{TM}$ UTI agar plates with: i) vancomycin (1 mg/L) and AMC (256 mg/L) to
595 detect the donor; ii) vancomycin (1 mg/L) and chloramphenicol (50 mg/L) to detect recipients; and
596 iii) vancomycin (1 mg/L), AMC (256 mg/L) and chloramphenicol (50 mg/L) to determine the
597 presence of transconjugants. We calculated the colonization levels of the members of each
598 conjugation assay with the following formula:

599 $$CFU/mg_{donor,recipient} = \frac{CFU_{donor,recipient} - CFU_{transconjugants}}{mg_{feces}}$$

600 From the levels of recipients and transconjugants we calculated the conjugation frequencies per
601 recipient as described before in the *in vitro* protocol. At 48 h post inoculation, after fresh fecal
602 samples collection, we sacrificed mice and obtained samples of cecum content by manual
603 extrusion. We performed sample processing, bacterial levels determination and conjugation
604 frequencies determination as described above.

605 **DNA extraction and genome sequencing.** We isolated the genomic DNA of the strains used in
606 this work using the Wizard genomic DNA purification kit (Promega, WI, USA) and quantified using
607 the Qubit 4 fluorometer (ThermoFisher Scientific, MA, USA). Whole genome sequencing was
608 performed at the Wellcome Trust Centre for Human Genetics (Oxford, UK) using the Illumina
609 HiSeq4000 or NovaSeq6000 platforms with 125 or 150 base pair (bp) paired-end reads,
610 respectively. Read data is available under the BioProject PRJNA803387.

611 **Processing of sequencing data.** All Illumina reads were trimmed with a quality threshold of 20
612 and reads shorter than 50 bp and adapters were removed using Trim Galore v0.6.6
613 (https://github.com/FelixKrueger/TrimGalore). PF and TC genomes were *de novo* assembled with
614 SPAdes v3.15.2 (51) in --isolate mode and with the --cov-cutoff flag set to auto. Assembly quality
615 was assessed with QUAST v5.0.2 (52). TC were confirmed to correspond to their PF strain by
616 checking mutations and plasmid content with Snippy v4.6.0 (https://github.com/tseemann/snippy)
617 and ABRicate v1.0.1 (PlasmidFinder database, https://github.com/tseemann/abricate),
618 respectively. Snippy was also used to confirm isogenicity of the acquired pOXA-48 plasmids.
619 Multilocus sequence typing was performed with MLST v2.21.0
620 (https://github.com/tseemann/mlst).

621 **Construction of phylogenetic trees.** Mash distance phylogenies were constructed for the 25 *E.*
622 *coli* and 25 *Klebsiella* spp. PF strains from their whole-genome assemblies using mashtree v1.2.0
623 (53) with a bootstrap of 100 (Fig. S10).

624 **Plasmid copy number (PCN) estimation.** PCN of pOXA-48 was determined for the 33 TC
625 strains and the 200 wild-type *E. coli* and *Klebsiella* spp. R-GNOSIS strains (BioProject
626 PRJNA626430) carrying pOXA-48 variants sharing 72% of the pOXA-48_K8 core genome (32,
627 36). PCN was estimated from read coverage data as the ratio of plasmid median coverage by
628 chromosome median coverage (54, 55). Since the genome assemblies are fragmented, the
629 median coverage of the chromosome was calculated from the first three, largest contigs (total
630 size sum of first three contigs 0.3-4.0 Mb), which were confirmed to correspond to chromosomal
631 sequences by using BLASTn against the NCBI nr nucleotide database. The median coverage of
632 pOXA-48 was calculated from the contig containing the IncL replicon, as identified with ABRicate
633 v1.0.1 with the PlasmidFinder database, which generally corresponds to the largest pOXA-48
634 contig (size 11.0-59.8 Kb). For computing the PCN, the Illumina trimmed reads were first mapped

635 to their respective genome assembly using BWA MEM v0.7.17 (56). Strain K25 from the wild-type
636 pOXA-48-carrying collection was removed from the analysis due to truncated reads. Samtools
637 depth v1.12 (57) with the -a flag was used to obtain read depths at each genomic position and
638 the median read coverage for pOXA-48 and chromosome was computed with GNU datamash
639 v1.4 (gnu.org/software/datamash).

640 **Comparative genomic analysis of recipient strains.** We analyzed the genomes of the recipient
641 strains to find traits that could explain the observed differences in pOXA-48 acquisition. First, the
642 draft genomes of the 20 recipients and three donors (*E. coli* ST10 C165 and *K. pneumoniae* ST11
643 K93 from Bioproject PRJNA626430; for *E. coli* β3914, the sequence of the ancestral K-12 strain,
644 NC_000913.3) were annotated with Prokka v1.14.6 (58) with default settings. A summary of the
645 results can be found in Table S3.

646 Restriction-modification (RM) systems were searched using two approaches. First, the protein
647 sequences of the recipient and donor strains were blasted against the protein "gold standard"
648 REBASE database (downloaded February 2022, (59)) using BLASTp v2.9.0 (60). The results
649 were filtered with a criteria based on (61). Briefly, hits with type I and IIG RM systems were kept
650 if the percentage of identity and alignment was 100%, since it was observed that recognition sites
651 varied between enzymes with only a few mismatches. For type II systems, a threshold of 70%
652 identity and 90% alignment was used, as it was previously reported that these systems with
653 identity over 55% generally share the same target motifs. For type III and type IV this threshold
654 was higher, as reported in the same study, and was set at 90% identity and 90% alignment. After
655 filtering, some proteins had hits with more than one enzyme. For these cases, the best hit or the
656 hit with the enzyme of the corresponding organism (*E. coli* or *Klebsiella* spp.) was kept. The
657 DefenseFinder webserver (accessed February 2022, (62, 63)) was also used to search for RM
658 systems in the proteomes of recipients and donors. Then, the REBASE hits and the RM systems
659 detected by DefenseFinder were unified by protein ID. Enzymes or RM systems present in all
660 strains were discarded, since they would not explain differences in conjugation frequencies
661 between isolates. Finally, only complete RM systems that were not present in the donor strains
662 were retained for each recipient-donor combination, since the donor would be conferring
663 protection to pOXA-48 against equivalent systems of the recipient. Complete type I systems
664 comprise a restriction enzyme (REase), a methylase (MTase) and a specificity (S) subunit. Type

665 II systems include at least a REase and a MTase. No type III systems were detected, and type IV
666 systems are normally composed of one or two proteins. Donor and recipient systems were
667 regarded as similar if they shared the same recognition sequence or if a BLASTp alignment of
668 the enzymes followed the previous criteria of identity and alignment percentage per type of
669 system. The same method was applied for comparing the final systems between recipient strains,
670 and similar systems within each type were given the same letter code identifying the RM system
671 subtype (Fig. S15, Table S3).

672 Clustered regularly interspaced short palindromic repeats (CRISPRs) were identified in the
673 nucleotide sequences of the recipient strains with the DefenseFinder webserver. The spacer
674 sequences were aligned to pOXA-48_K8 (MT441554) using the blastn-short function of BLASTn
675 v2.9.0 (60) and hits were then filtered by percentage of alignment. Other defense systems were
676 also detected with the DefenseFinder webserver and PADLOC v1.1.0 (database v1.3.0, (64)).

677 Plasmid incompatibility was investigated by identifying plasmid replicons using ABRicate v1.0.1
678 with the PlasmidFinder database.

679 Secretion systems were searched using the TXSScan models of MacSyFinder v1.0.5 (62, 65),
680 selecting the option "ordered_replicon" and linear topology. Only complete systems were
681 considered.

682 Capsular systems were identified using two software. First, *Klebsiella* capsules, which belong to
683 the Wzx/Wzy-dependent group I capsular systems, were identified with Kaptive v2.0.0 (66), using
684 the K locus primary reference and default parameters. The presence of *Klebsiella* capsules was
685 assigned when the confidence level of the matches was above "good", as recommended by the
686 authors. Other capsular systems from groups I (Wzx/Wzy-dependent), II and III (ABC-dependent),
687 IV, synthase-dependent (cps3-like and hyaluronic acid) and PGA (Poly-γ-d-glutamate) were
688 searched using MacSyFinder v1.0.5 with the CapsuleFinder for diderms models, indicating
689 "ordered_replicon" as database type and linear topology (62, 67). Only systems reported as
690 complete were considered. In the cases where *Klebsiella* capsular loci were also identified by
691 CapsuleFinder as group I capsules, analyses were performed with the Kaptive output. To assess
692 the similarity of the different sets of capsular loci between strains, a weighted gene repertoire
693 relatedness (wGRR) score was calculated as in (68). For this, significant sequence similarities (e-

694 value <10^{-4}, identity ≥35%, coverage ≥50%) among all pairs of proteins in the capsular loci were

695 searched using MMSeqs2 (Nature Biotechnology release, August 2017, (69)) with the sensitivity

696 parameter set to 7.5. The best bi-directional hits between pairs of capsule loci sets were then

697 used to compute the wGRR as:

698 $$wGRR_{A,B} = \Sigma_i \frac{id(A_i, B_i)}{min(A, B)}$$

699 where $id(A_i, B_i)$ is the sequence identity between each pair *i* of homologous proteins in *A* and *B*,

700 and *min(A, B)* is the number of proteins of the capsule loci set encoding the fewest proteins (*A* or

701 *B*). The wGRR takes values between 0 (no homologous proteins between capsule loci sets) and

702 1 (all genes of the smallest capsule loci set have an identical homologous in the loci set of the

703 other strain), representing the fraction of homologs in the smallest of the two capsule loci set

704 weighted by their sequence similarity. Protein sequences of the *Klebsiella* capsular loci were

705 obtained from Prokka annotations of the operon nucleotide sequences output by Kaptive. All

706 proteins between the borders of CapsuleFinder complete systems were included.

707 **Analysis of capsular systems in a database.** The database comprised the genomes of 730 *K.*

708 *pneumoniae* and 1,585 *E. coli* downloaded from the NCBI RefSeq database of high quality

709 complete non-redundant genomes (retrieved from ftp://ftp.ncbi.nlm.nih.gov/genomes/refseq/ on

710 March 2021; Table S4) (70). pOXA-48-carrying strains were identified in the RefSeq database

711 when the best, largest BLASTn hit between the sequence of pOXA-48_K8 (MT441554) and the

712 target plasmid had >95% identity and >10 Kb alignment, and when the plasmid sequence

713 contained the pOXA-48 IncL replicon and the bla_{OXA-48} gene as detected by ABRicate with the

714 PlasmidFinder and ResFinder databases. The plasmids of 6 *E. coli* and 46 *K. pneumoniae* strains

715 met this criteria, which had lengths between 50.6-74.2 Kb (average 64.0 Kb; Table S4). Kaptive

716 and CapsuleFinder were used as previously described to search for *Klebsiella*-derived capsules

717 and capsular systems, respectively, and to discard non-capsulated strains (15 *K. pneumoniae*

718 strains).

719 Associations between the presence of *Klebsiella*-derived capsules and pOXA-48- or plasmid-

720 carriage were analyzed building 2x2 contingency tables. Significant interactions ($P < 0.05$, Fisher

721 exact test) were then corrected for phylogenetic dependency, i.e. the tendency of closely related

722 strains to share the same traits. For this, a set of 128 HMM profiles (Pfam release 35, Table S5)
723 of conserved bacterial single copy genes, described in (71) and curated in (72), were identified in
724 the RefSeq strains and an *Enterobacter cloacae* outgroup (accession number
725 GCF_003204095.1) using HMMER v3.3 (option --cut_ga) (73). Hits were filtered by score using
726 the cutoffs reported in (65), resulting in 127 gene markers present in >90% of strains. Protein
727 sequences of each family were aligned with MAFFT v7.453 (option --auto) (74) and alignments
728 were trimmed with trimAl v1.4.rev15 (75). IQ-TREE v1.6.12 (76) was used to infer two
729 phylogenetic trees from the concatenated alignments (the first including all capsulated strains,
730 and the second including only *E. coli* strains, both with the *E. cloacae* outgroup) with best
731 evolutionary model selection and 1000 ultrafast bootstrap. Trees were rooted and rescaled to a
732 total height of 1. Phylogenetic logistic regression for each significant association was performed
733 with the function *phyloglm* from the *phylolm* v2.6.4 R package (77), fitting a logistic MPLE model
734 with 100 independent bootstrap replicates.

735 **Mathematical model and simulations of polymicrobial communities.** A detailed description
736 of the population dynamics model and the computational simulations can be found in the
737 Supporting Information (SI Text). All code and data used is available at https://github.com/ccg-
738 esb/EvK.

739 **Statistical analyses.** All statistical analyses were performed with R v4.2.2 (www.R-project.org).
740 Packages *ggplot2* v3.3.6, *ggpubr* v0.4.0 *pheatmap* v1.0.12, *RColorBrewer* v1.1-3, *ggsignif* v0.6.3
741 and *tidyverse* v1.3.1 were used for data manipulation and representation. R base packages were
742 used for statistical tests. Normality of the data was assessed with the Shapiro-Wilk test. To
743 analyze the differences in initial (PF) and final (TC) MIC of antibiotics and PCN between *E. coli*
744 and *Klebsiella* spp. a Wilcoxon sum-rank test was used. To analyze the differences between the
745 members of each recipient couple in the pairwise conjugation experiments (Shapiro-Wilk
746 normality test, $P < 0.01$ in all cases), the non-parametric Wilcoxon paired signed-rank test was
747 used. To determine differences between receptor species in the classical and pooled recipient
748 conjugation experiments, as well as in *in vivo* conjugation assays (Shapiro-Wilk normality test, P
749 < 0.01 in all cases), the non-parametric Kruskal-Wallis test was performed. Correlations were
750 performed with the Spearman's rank test. Phylogenetic analyses were performed with *ape* v5.6-
751 2, *phytools* v1.0-3 and *phylolm* v2.6.4 packages.

752 **Data and code availability.** Sequencing data generated in this study is available in the Sequence
753 Read Archive (SRA) under the BioProject PRJNA803387. The R-GNOSIS sequences were
754 generated in (32) and a subset of strains were selected as in (36) (see Methods). All source data
755 is provided as Supporting Information. The code generated during the study along with detailed
756 bioinformatic methods is available at https://github.com/LaboraTORIbio/super-sinks and
757 https://github.com/ccg-esb/EvK.

758

759 **Acknowledgements**

760 This work was supported by the European Research Council (ERC) under the European Union's
761 Horizon 2020 research and innovation programme (ERC grant no. 757440-PLASREVOLUTION)
762 and by the Instituto de Salud Carlos III (PI19/00749) cofunded by the European Development
763 Regional Fund 'A way to achieve Europe'. The R-GNOSIS project received financial support from
764 the European Commission (grant no. R-GNOSIS-F P7-HEALTH-F3-2011-282512). C.U. was
765 supported by a grant from MICINN (PID2020-120292RB-I00). We appreciate Andrea Fernandez
766 Duque's contribution in creating the visual illustrations.

767 **Bibliography**
768

769 1. J. P. Gogarten, J. P. Townsend, Horizontal gene transfer, genome innovation and evolution.
770 Nat Rev Microbiol 3, 679–687 (2005).
771 2. A. San Millan, R. C. MacLean, Fitness Costs of Plasmids: a Limit to Plasmid Transmission.
772 Microbiol. Spectr. 5 (2017).
773 3. D. A. Baltrus, Exploring the costs of horizontal gene transfer. Trends Ecol Evol 28, 489–495
774 (2013).
775 4. K. Z. Coyte, et al., Horizontal gene transfer and ecological interactions jointly control
776 microbiome stability. PLOS Biol. 20, e3001847 (2022).
777 5. M. A. Brockhurst, E. Harrison, Ecological and evolutionary solutions to the plasmid paradox.
778 Trends Microbiol. (2021) https:/doi.org/10.1016/j.tim.2021.11.001.
779 6. M. J. Bottery, Ecological dynamics of plasmid transfer and persistence in microbial
780 communities. Curr. Opin. Microbiol. 68, 102152 (2022).
781 7. F. M. Stewart, B. R. Levin, The Population Biology of Bacterial Plasmids: A PRIORI
782 Conditions for the Existence of Conjugationally Transmitted Factors. Genetics 87, 209–228
783 (1977).
784 8. A. J. Lopatkin, et al., Persistence and reversal of plasmid-mediated antibiotic resistance. Nat.
785 Commun. 8, 1689 (2017).
786 9. P. E. Turner, V. S. Cooper, R. E. Lenski, TRADEOFF BETWEEN HORIZONTAL AND
787 VERTICAL MODES OF TRANSMISSION IN BACTERIAL PLASMIDS. Evol. Int. J. Org. Evol.
788 52, 315–329 (1998).
789 10. J. H. Bethke, et al., Vertical and horizontal gene transfer tradeoffs direct plasmid fitness. Mol.
790 Syst. Biol., e11300 (2022).
791 11. F. Benz, A. R. Hall, Host-specific plasmid evolution explains the variable spread of clinical
792 antibiotic-resistance plasmids" Proc. Natl. Acad. Sci. 120 (15) e2212147120 (2023)
793 12. Jordt, H., et al. Coevolution of host–plasmid pairs facilitates the emergence of novel
794 multidrug resistance. Nat. Ecol. Evol. 4, 863–869 (2020)
795 13. C. T. Bergstrom, M. Lipsitch, B. R. Levin, Natural selection, infectious transfer and the
796 existence conditions for bacterial plasmids. Genetics 155, 1505–1519 (2000).
797 14. L. N. Lili, N. F. Britton, E. J. Feil, The persistence of parasitic plasmids. Genetics 177, 399–
798 405 (2007).
799 15. J. M. Ponciano, L. De Gelder, E. M. Top, P. Joyce, The population biology of bacterial
800 plasmids: a hidden Markov model approach. Genetics 176, 957–968 (2007).
801 16. J. C. R. Hernández-Beltrán, A. San Millán, A. Fuentes-Hernández, R. Peña-Miller,
802 Mathematical Models of Plasmid Population Dynamics. Front. Microbiol. 12, 3389 (2021).
803 17. A. San Millan, et al., Positive selection and compensatory adaptation interact to stabilize
804 non-transmissible plasmids. Nat Commun 5, 5208 (2014).
805 18. J. P. J. Hall, A. J. Wood, E. Harrison, M. A. Brockhurst, Source–sink plasmid transfer
806 dynamics maintain gene mobility in soil bacterial communities. Proc. Natl. Acad. Sci. 113,
807 8260–8265 (2016).
808 19. L. Li, et al., Plasmids persist in a microbial community by providing fitness benefit to multiple
809 phylotypes. ISME J. 14, 1170–1181 (2020).
810 20. T. Dimitriu, L. Marchant, A. Buckling, B. Raymond, Bacteria from natural populations transfer
811 plasmids mostly towards their kin. Proc. R. Soc. B 286, 20191110 (2019).
812 21. J. H. Bethke, et al., Environmental and genetic determinants of plasmid mobility in
813 pathogenic *Escherichia coli*. Science Advances. 6, 4 (2020).
814 22. J. A. Gama, J. Kloos, P. J. Johnsen, Ø. Samuelsen, Host dependent maintenance of a
815 blaNDM-1-encoding plasmid in clinical Escherichia coli isolates. Sci. Rep. 10, 9332 (2020).
816 23. S. Dunn, L. Carrilero, M. Brockhurst, A. McNally, Limited and Strain-Specific Transcriptional
817 and Growth Responses to Acquisition of a Multidrug Resistance Plasmid in Genetically
818 Diverse Escherichia coli Lineages. mSystems. 6 (2021).
819 24. S. Heß, D. Kneis, M. Virta, T. Hiltunen, The spread of the plasmid RP4 in a synthetic

820 bacterial community is dependent on the particular donor strain. FEMS Microbiol. Ecol. 97
821 (2021).
822 25. J. Cairns, L. Ruokolainen, J. Hultman, M. Tamminen, M. Virta, T. Hiltunen, Ecology
823 determines how low antibiotic concentration impacts community composition and horizontal
824 transfer of resistance genes. Commun. Biol. 1, 35 (2018).
825 26. S. R. Partridge, S. M. Kwong, N. Firth, S. O. Jensen, Mobile genetic elements associated with
826 antimicrobial resistance. Clin. Microbiol. Rev. 31 (2018).
827 27. C. J. L. Murray, et al., Global burden of bacterial antimicrobial resistance in 2019: a
828 systematic analysis. The Lancet (2022) https:/doi.org/10.1016/S0140-6736(21)02724-0.
829 28. WHO, List of bacteria for which new antibiotics are urgently needed
830 https://www.who.int/news/item/27-02-2017-who-publishes-list-of-bacteria-for-which-new-
831 antibiotics-are-urgently-needed (January 3, 2023).
832 29. A. Cassini, et al., Attributable deaths and disability-adjusted life-years caused by infections
833 with antibiotic-resistant bacteria in the EU and the European Economic Area in 2015: a
834 population-level modelling analysis. Lancet Infect. Dis. 19, 56–66 (2019).
835 30. J. D. D. Pitout, G. Peirano, M. M. Kock, K.-A. Strydom, Y. Matsumura, The Global
836 Ascendency of OXA-48-Type Carbapenemases. Clin. Microbiol. Rev. 33, e00102-19 (2019).
837 31. S. Redondo-Salvo, et al., Pathways for horizontal gene transfer in bacteria revealed by a
838 global map of their plasmids. Nat. Commun. 11, 3602 (2020).
839 32. R. León-Sampedro, et al., Pervasive transmission of a carbapenem resistance plasmid in the
840 gut microbiota of hospitalized patients. Nat. Microbiol. 6, 606–616 (2021).
841 33. S. David, et al., Epidemic of carbapenem-resistant Klebsiella pneumoniae in Europe is
842 driven by nosocomial spread. Nat. Microbiol. 4, 1919–1929 (2019).
843 34. A. Alonso-del Valle, et al., Variability of plasmid fitness effects contributes to plasmid
844 persistence in bacterial communities. Nat. Commun. 12, 2653 (2021).
845 35. A. San Millan, J. A. Escudero, D. R. Gifford, D. Mazel, R. C. MacLean, Multicopy plasmids
846 potentiate the evolution of antibiotic resistance in bacteria. Nat. Ecol. Evol. 1, 10 (2016).
847 36. J. DelaFuente, et al., Within-patient evolution of plasmid-mediated antimicrobial resistance.
848 Nat. Ecol. Evol. 6, 1980–1991 (2022).
849 37. L. Simonsen, D. M. Gordon, F. M. Stewart, B. R. Levin. Estimating the rate of plasmid
850 transfer: an end-point method. J Gen Microbiol. 136, 2319–2325 (1990).
851 38. O. Kosterlitz, J. S. Huisman. Guidelines for the estimation and reporting of plasmid
852 conjugation rates. Plasmid. 126, 102685 (2023).
853 39. R. Fernandez-Lopez, I. del Campo, C. Revilla, A. Cuevas, F. de la Cruz, Negative Feedback
854 and Transcriptional Overshooting in a Regulatory Network for Horizontal Gene Transfer.
855 PLoS Genet. 10, e1004171 (2014).
856 40 A. Djukovic, et al., Lactobacillus supports Clostridiales to restrict gut colonization by of 1,777
857 Extended-Spectrum Beta-Lactamase-Producing Klebsiella pneumoniae multidrug- resistant
858 Enterobacteriaceae. (2022). Nat. Commun. 13, 5617 (2022).
859 41. M. Haudiquet, A. Buffet, O. Rendueles, E. P. C. Rocha, Interplay between the cell envelope
860 and mobile genetic elements shapes gene flow in populations of the nosocomial pathogen
861 Klebsiella pneumoniae. PLoS Biol. 19, e3001276 (2021).
862 42. M. Haudiquet, et al., Capsules and their traits shape phage susceptibility and plasmid
863 conjugation efficiency. BioRxiv. (2023).
864 43. A. Fernandez-Calvet et al., The distribution of fitness effects of plasmid pOXA-48 in clinical
865 enterobacteria. Microbiol. 169(7) (2023).
866 44. K. L. Wyres, et al. Emergence and rapid global dissemination of CTX-M-15-associated
867 Klebsiella pneumoniae strain ST307. J. Antimicrob. Chemother. 74, 577–581 (2019).
868 45. S. W. Long, et al., Population Genomic Analysis Isolates, Houston, Texas: Unexpected
869 Abundance of Clonal Group 307. MBio. 8(3):e00489-17 (2017).
870 46. J. E. Cañada-García et al., CARB-ES-19 Multicenter Study of Carbapenemase-Producing
871 Klebsiella pneumoniae and Escherichia coli From All Spanish Provinces Reveals
872 Interregional Spread of High-Risk Clones Such as ST307/OXA-48 and ST512/KPC-3. Front.

873 Microbiol. 13:918362 (2022).
874 47. F. Le Roux, J. Binesse, D. Saulnier, D. Mazel, Construction of a Vibrio splendidus Mutant
875 Lacking the Metalloprotease Gene vsm by Use of a Novel Counterselectable Suicide Vector.
876 Appl. Environ. Microbiol. 73, 777–784 (2007).
877 48. I. Wiegand, K. Hilpert, R. E. W. Hancock, Agar and broth dilution methods to determine the
878 minimal inhibitory concentration (MIC) of antimicrobial substances. Nat. Protoc. 3, 163–175
879 (2008).
880 49. M. Agarwal, R. S. Rathore, A. Chauhan, A Rapid and High Throughput MIC Determination
881 Method to Screen Uranium Resistant Microorganisms. Methods Protoc. 3, 21 (2020).
882 50. M. Carlier, A. G. Verstraete, J. J. De Waele, V. Stove, Stability of amoxicillin and
883 amoxicillin/clavulanic acid reconstituted in isotonic saline. J. Chemother. 29, 54–56 (2017).
884 51. A. Bankevich, et al., SPAdes: a new genome assembly algorithm and its applications to
885 single-cell sequencing. J. Comput. Biol. J. Comput. Mol. Cell Biol. 19, 455–477 (2012).
886 52. A. Gurevich, V. Saveliev, N. Vyahhi, G. Tesler, QUAST: quality assessment tool for genome
887 assemblies. Bioinforma. Oxf. Engl. 29, 1072–1075 (2013).
888 53. L. S. Katz, et al., Mashtree: a rapid comparison of whole genome sequence files. J. Open
889 Source Softw. 4, 1762 (2019).
890 54. H. Wang, et al., Increased plasmid copy number is essential for Yersinia T3SS function and
891 virulence. Science 353, 492–495 (2016).
892 55. P. K. Jangir, et al., Pre-existing chromosomal polymorphisms in pathogenic E. coli potentiate
893 the evolution of resistance to a last-resort antibiotic. eLife 11, e78834 (2022).
894 56. H. Li, Aligning sequence reads, clone sequences and assembly contigs with BWA-MEM
895 (2013) https:/doi.org/10.48550/arXiv.1303.3997 (January 18, 2023).
896 57. P. Danecek, et al., Twelve years of SAMtools and BCFtools. GigaScience 10, giab008
897 (2021).
898 58. T. Seemann, Prokka: rapid prokaryotic genome annotation. Bioinformatics 30, 2068–2069
899 (2014).
900 59. R. J. Roberts, T. Vincze, J. Posfai, D. Macelis, REBASE—a database for DNA restriction
901 and modification: enzymes, genes and genomes. Nucleic Acids Res. 38, D234–D236 (2010).
902 60. S. F. Altschul, W. Gish, W. Miller, E. W. Myers, D. J. Lipman, Basic local alignment search
903 tool. J. Mol. Biol. 215, 403–410 (1990).
904 61. P. H. Oliveira, M. Touchon, E. P. C. Rocha, Regulation of genetic flux between bacteria by
905 restriction–modification systems. Proc. Natl. Acad. Sci. 113, 5658–5663 (2016).
906 62. S. S. Abby, B. Néron, H. Ménager, M. Touchon, E. P. C. Rocha, MacSyFinder: a program to
907 mine genomes for molecular systems with an application to CRISPR-Cas systems. PLOS
908 ONE 9, e110726 (2014).
909 63. F. Tesson, et al., Systematic and quantitative view of the antiviral arsenal of prokaryotes.
910 Nat. Commun. 13, 2561 (2022).
911 64. L. J. Payne, et al., Identification and classification of antiviral defence systems in bacteria
912 and archaea with PADLOC reveals new system types. Nucleic Acids Res. 49, 10868–10878
913 (2021).
914 65. S. S. Abby, et al., Identification of protein secretion systems in bacterial genomes. Sci. Rep.
915 6, 23080 (2016).
916 66. M. M. C. Lam, R. R. Wick, L. M. Judd, K. E. Holt, K. L. Wyres, Kaptive 2.0: updated capsule
917 and lipopolysaccharide locus typing for the Klebsiella pneumoniae species complex. Microb.
918 Genomics 8, 000800 (2022).
919 67. O. Rendueles, M. Garcia-Garcerà, B. Néron, M. Touchon, E. P. C. Rocha, Abundance and
920 co-occurrence of extracellular capsules increase environmental breadth: Implications for the
921 emergence of pathogens. PLOS Pathog. 13, e1006525 (2017).
922 68. J. A. M. de Sousa, A. Buffet, M. Haudiquet, E. P. C. Rocha, O. Rendueles, Modular
923 prophage interactions driven by capsule serotype select for capsule loss under phage
924 predation. ISME J. 14, 2980–2996 (2020).
925 69. M. Steinegger, J. Söding, MMseqs2 enables sensitive protein sequence searching for the

926 analysis of massive data sets. Nat. Biotechnol. 35, 1026–1028 (2017).
927 70. D. H. Haft, et al., RefSeq: an update on prokaryotic genome annotation and curation. Nucleic
928 Acids Res. 46, D851–D860 (2018).
929 71. C. Rinke, et al., Insights into the phylogeny and coding potential of microbial dark matter.
930 Nature 499, 431–437 (2013).
931 72. C. d'Humières, et al., A simple, reproducible and cost-effective procedure to analyse gut
932 phageome: from phage isolation to bioinformatic approach. Sci. Rep. 9, 11331 (2019).
933 73. S. R. Eddy, Accelerated Profile HMM Searches. PLOS Comput. Biol. 7, e1002195 (2011).
934 74. K. Katoh, D. M. Standley, MAFFT Multiple Sequence Alignment Software Version 7:
935 Improvements in Performance and Usability. Mol. Biol. Evol. 30, 772–780 (2013).
936 75. S. Capella-Gutiérrez, J. M. Silla-Martínez, T. Gabaldón, trimAl: a tool for automated
937 alignment trimming in large-scale phylogenetic analyses. Bioinforma. Oxf. Engl. 25, 1972–
938 1973 (2009).
939 76. L.-T. Nguyen, H. A. Schmidt, A. von Haeseler, B. Q. Minh, IQ-TREE: A Fast and Effective
940 Stochastic Algorithm for Estimating Maximum-Likelihood Phylogenies. Mol. Biol. Evol. 32,
941 268–274 (2015).
942 77. L. si Tung Ho, C. Ané, A linear-time algorithm for Gaussian and non-Gaussian trait evolution
943 models. Syst. Biol. 63, 397–408 (2014).
944
945